Neurological Surgery and Anatomy 2025, 2(3): 71-78, e-ISSN: 2966-0696
DOI: 10.37085/ns&a.2025.13

Original

Topographic significance of the parietal foramen in identifying intracranial vascular and parenchymal structures

Pedro Brainer-Lima[1], Alessandra Brainer-Lima[2], Maria Rosana Ferreira[1], Paulo Brainer-Lima[3], Marcelo Moraes Valença[1,4]

[1]Federal University of Pernambuco, Recife, Pernambuco, Brazil
[2]Departament of Radiology, University Cardiology Emergency Department of Pernambuco, Prof. Luiz Tavares, Recife, Pernambuco, Brazil
[3]Restoration Hospital, Recife, Pernambuco, Brazil
[4]Esperança Hospital Recife, D'Or São Luiz, Recife, Pernambuco, Brazil

Objective
This study aimed to define the location of the parietal foramina (PF) in relation to skull landmarks and correlate the PF with cerebral and vascular structures to optimize neurosurgical procedures within the intracranial compartment.
Methods
Two hundred thirty-eight parietal bones, studied using magnetic resonance imaging (MRI) in 119 patients, were reviewed. The cephalometric points, including inion, bregma, sagittal suture, and lambda, were used as anatomical references to locate the PF and define its anatomical relationships to parenchymal cerebral structures, particularly some eloquent areas.
Results
The PF was identified in the MRI in 83 of the 119 individuals (69.7%) and was located at a distance of 9.5 ± 0.8 cm (mean ± SD) posteriorly and 0.9 ± 0.3 cm laterally to the bregma. In over 90% of cases, the PF was located within a 2 cm radius of the mean value of the bregma-PF distance. 88% of the 62 left PFs were situated within 1 cm, laterally to the left margin of the superior sagittal sinus (SSS). 60% of the right PF were located within 1.3 cm laterally from the right margin of the SSS, while 40% were directly above the SSS.
Conclusion
The PF should be considered a reliable reference point for the SSS during its course through the parietal lobe, as its consistency surpasses that of other commonly used landmarks, such as the sagittal suture and midline. Identified in approximately 70% of individuals, the PF demonstrates a relatively constant anatomical relationship with the SSS. Recognizing this foramen is crucial for neurosurgeons operating in the parietal region, not only to avoid iatrogenic injury to the emissary veins, arteries, and nerves that traverse it—which could lead to complications such as air embolism—but also to provide a more dependable guide for navigating the SSS. Surgeons should remain aware of the PF's frequency (69.7%), its typical location superolateral to the lambda, and its stable topographic association with underlying structures.

Keywords: Parietal foramina, Landmarks, Vascular, Neurosurgical procedures, Magnetic Resonance Imaging, Skull

Edited by:
Carolina Martins

Pedro Brainer-Lima
pedro.brainerlima@ufpe.br

Received: August 30, 2025
Revised: September 19, 2025
Accepted: October 21, 2025

Introduction

The parietal foramen (PF) is a small natural canal located in the posterior portion of the parietal bone, typically positioned 2–5 mm lateral to the sagittal suture (1–7). It serves as a passage for an arterial anastomosis between the middle meningeal and scalp arteries, as well as for an emissary vein connecting intracranial venous structures—such as the superior sagittal sinus and diploic veins—with the extracranial venous system (3,8). These vascular connections largely determine the anatomy and localization of the PF. Its occurrence is variable: the PF may be absent, unilateral, or, more commonly, bilateral in more than half of individuals. Previous studies on dry skulls have reported its presence in approximately 60–80% of cases (2,5,9,10).

It is thought that the valveless emissary vein traversing the parietal foramen serves both vascular and physiological roles in regulating intracranial temperature and pressure. Owing to its capacity for bi-directional blood flow, this vessel facilitates exchange between the intra- and extracranial venous systems, allowing blood to circulate in either direction depending on pressure gradients and thermo-regulatory demands (11–13). A study demonstrated that during hyperthermia, blood flow through the emissary vein increases from the scalp to the brain, whereas under hypothermic conditions the flow either ceases or reverses, establishing a brain-to-scalp direction (12). It appears that relatively high frequencies of the parietal foramen are observed only in extant humans. In association with skull thinning, this trait was likely influenced by evolutionary and epigenetic factors (13). The increase in parietal and other cranial foramina may have been driven by practical evolutionary pressures such as the emergence of bipedality, brain enlargement, orthognathy (14) and the need for enhanced brain cooling, particularly as other venous pathways—such as the occipital and marginal sinuses—declined in frequency (13).

Parietal foramina can be reliably identified both in radiological studies and during in vivo examination (3). Their location may serve as a useful surgical landmark for estimating anatomical relationships with parenchymal structures, particularly eloquent areas such as the angular gyrus. This knowledge can guide the placement of a craniotomy window and orient surgical maneuvers around the superior sagittal sinus (SSS), thereby minimizing the risk of venous injury—an uncommon but potentially fatal complication (6). Improperly performed craniotomies in the parietal region, without consideration of the parietal foramen (PF), may damage the emissary vein and become a potential source of air embolism (4). Thus, physicians should recognize the presence of the PF and its vascular anastomoses in order to navigate the parietal region more safely and minimize the risk of iatrogenic injury to critical vascular structures.

Although the parietal foramen has been described in previous literature, reports focusing specifically on its anatomical correlations remain scarce, resulting in limited and often insufficient information about this structure. Previous studies diverged in landmarks used to locate the PF, applying either inion (6), bregma (7) or lambda (8). The absence of a standardized method for localizing the PF hampers both its accurate clinical application and future research. Furthermore, because most prior investigations have relied on cadaveric studies, correlations between the PF and parenchymal brain structures have not been adequately established.

The inion, bregma, and lambda are anatomical landmarks commonly employed in surgical planning. These points are easily accessible, stable, and therefore serve as valuable references. A comparative analysis of these landmarks is necessary to determine which is most reliable for identifying the PF, which in turn can guide the accurate localization of nearby eloquent structures such as the angular gyrus, central sulcus, and SSS. This study focuses on the use of MRI to assess the reliability of the PF as a landmark for parenchymal and venous structures, thereby providing clinicians with a safer and more precise method to navigate the parietal lobe and the SSS.

Methods

A total of 142 cerebral MRI examinations were analyzed. Only subjects without expansive intracranial processes (such as tumors, subacute ischemia, or hemorrhage) were included. After excluding 23 patients with anatomical disruptions, 119 cases were deemed suitable for morphometric assessment. Each patient was examined independently on the right and left sides. The mean age of the cohort was 58.9 years (range 18–80 years). Examinations were performed using a 1.5-T MR scanner equipped with an 8-channel head coil (Achieva02; Philips Medical Systems, Recife, Brazil). Contrast-enhanced imaging was obtained after intravenous infusion of gadolinium (0.1 mmol/kg) on a T1-weighted sequence, with sagittal coverage of the entire cranial vault. Acquisition parameters were as follows: repetition time, 6.983 ms; echo time, 3.162 ms; slice thickness, 1.0 mm; interslice gap, 0.5 mm; matrix, 256 × 256; flip angle, 8°; and scan duration, 5 min 19 s. All contrast-enhanced imaging data were transferred to OsiriX software (version 10.0.1) for analysis. In addition, 20 patients from the pool of 119 were randomly selected to undergo measurement of the squamous part of the occipital bone using CT scans. In cases of uncertainty, a consensus decision was reached through discussion between the primary investigator (P.T.B.) and a senior neuroradiologist with more than 15 years of experience (A.M.B.). The study was approved by the Ethics Committee for Research Involving Human Subjects at the Federal University of Pernambuco, Brazil (CAAE: 79464917.6.0000.5208). All procedures were carried out in accordance with relevant guidelines and regulations, and informed consent was obtained when required.

Measured parameters

The location of the PF was determined using external cranial landmarks, including the obelion, inion, bregma, and lambda (Figures 1-3). Morphometric measurements were obtained using OsiriX 10.0.1 software, with the exception of parameter #12, which was measured with Slicer 4.11.0. The following parameters were analyzed:

1. Vertical distance from the obelion to the lambda.
2. Horizontal distance from the obelion to the PF.
3. Distance from the obelion to the angular gyrus reference point on

the sagittal suture.
4. Distance from the PF to the bregma.
5. Distance from the PF to the inion.
6. Distance from the PF to the central sulcus.
7. Distance from the PF to the vertex.
8. Distance from the PF to the confluence of sinuses.
9. Distance from the PF to the eurion.
10. Distance from the angular gyrus to the PF.
11. Distance from the angular gyrus to the angular gyrus reference point on the sagittal suture.
12. Area of the squamous part of the occipital bone (measured using Slicer 4.11.0).
13. Distances from the PF to the margins of the SSS.

Statistical analysis

Statistical analyses were performed using SPSS software (version 18.0; SPSS Inc., Chicago, IL, USA). Normality of the data distribution was assessed using the Shapiro–Wilk test to determine whether parametric or nonparametric analyses were appropriate. Full heads were examined bilaterally in 83 patients, and laterality was assessed using the paired-samples t-test. Linear relationships between study parameters (#1 and #6, #1 and #5, and #1 and #4) were evaluated with Pearson's correlation test. The chi-square test was applied to assess the association between PF side distribution and sex. Statistical significance was set at $p < 0.05$. All results are presented as mean ± standard deviation (SD).

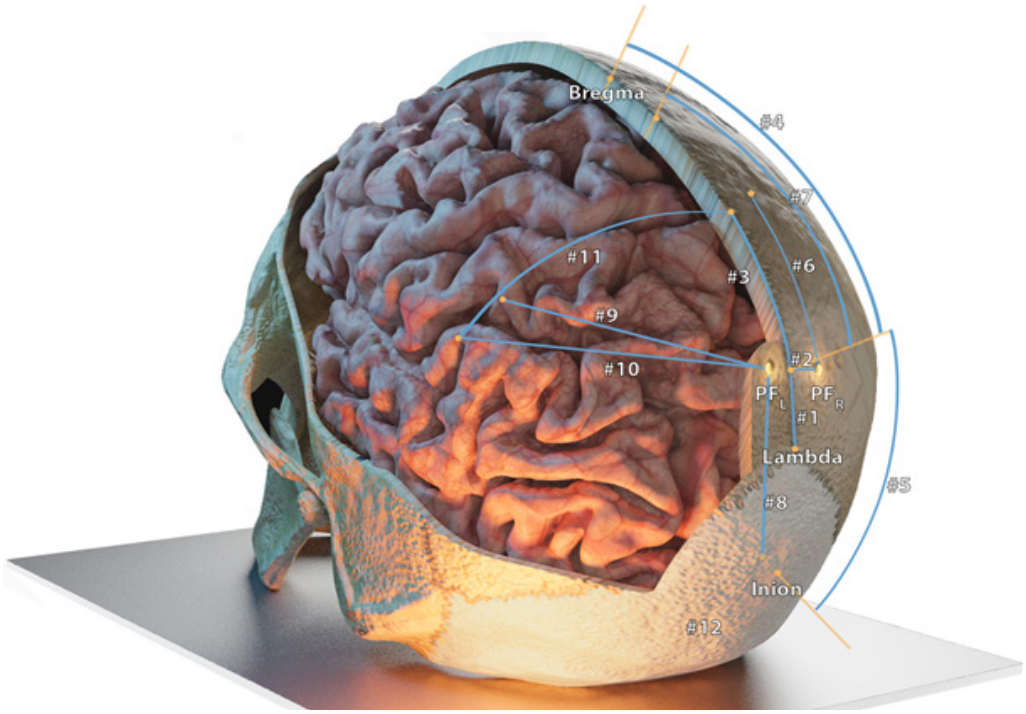

Figure 1. Illustration of the main parameters (#1–#12). PF, parietal foramen; PFR, right parietal foramen; PFL, left parietal foramen.

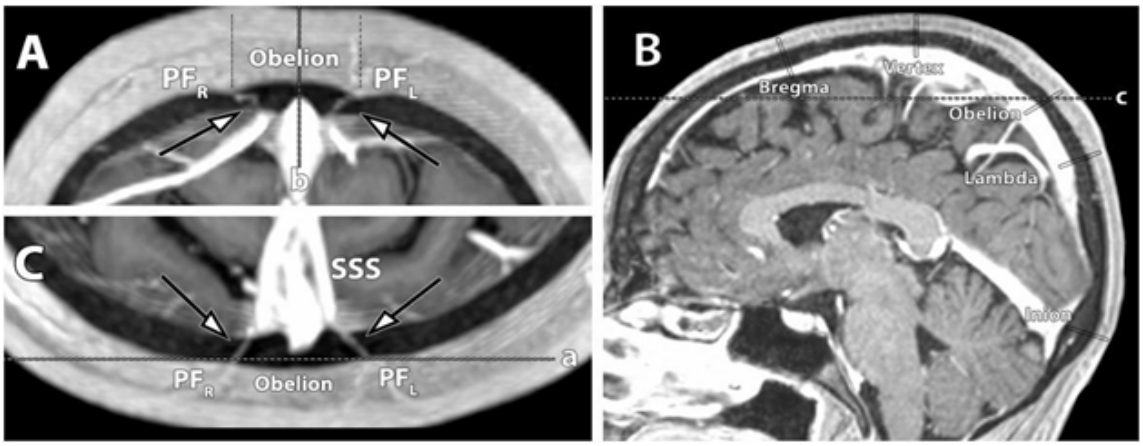

Figure 2. MRI studies demonstrating cranial and vascular landmarks. (A) Maximum intensity projection (MIP) of a 5-mm coronal slice, showing symmetrical right (PFR) and left (PFL) parietal foramina with their emissary veins (arrows), mirrored across the obelion. (B) Midline sagittal slice illustrating the spatial relationship of the principal midline cranial landmarks. (C) MIP of a 5-mm axial slice demonstrating emissary veins converging into the superior sagittal sinus (SSS). The dotted line indicates the slice level corresponding to the designated letter. Labels 'a', 'b', and 'c' mark the respective slice levels at which images 1A, 1B, and 1C were acquired.

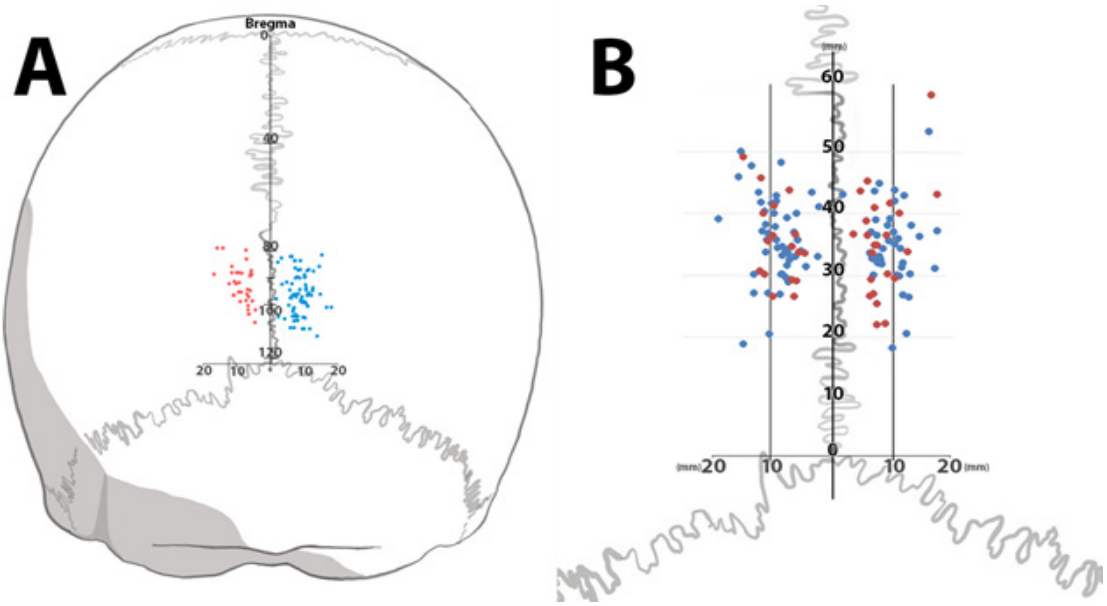

Figure 3. Schematic drawing showing the distribution of the parietal foramina (PF). No differences in distribution patterns were found between men and women. (A) Comparison of PF distribution measured from the bregma between men (blue) and women (red). Measures are presented regardless of laterality. (B) Comparison of right and left PF distribution according to sex (female = red, male = blue). Overall, 92.6% of PFs were located within a 20-mm radius of the mean value. Units in millimeters.

Results

Most measurements followed a normal distribution, except for those related to the distances between the margins of the SSS and the left or right PF (parameter #13). A significant laterality difference between the two sides was observed for parameter #13, as detailed in Table 1, along with the corresponding values, and is illustrated in Figure 2. All identified PFs traversed the entire cranial thickness as a single canal. On imaging, this appeared as an intensely enhanced straight or curvilinear structure crossing the foramen (Figure 2A–C).

Table 1. Measured parameters. Detailed descriptions are provided in the main text and in Figure 1. Units are expressed in millimeters, except for parameter 12 (mm²) and coefficients of variation (percentages). Parameters for which the paired-samples t-test showed no significant left–right laterality differences were grouped (n = 122). For parameters with significant laterality differences, values are presented separately for the left (n = 62) and right (n = 60) sides. Parameter 12 was assessed in n = 20 cases. AGyRSS, Angular Gyrus Reference point upon Sagittal Suture; #, parameter number

Anatomic parameter	#	Mean ± SD		Coefficient of variance (Left/Right)	
Distance from obelion to:					
Lambda	1	35.3 ± 6.9		19.6	
Parietal foramen	2	8.9 ± 3.1		34.7	
AGyRSS**	3	25.6 ± 10.6	34.9 ± 10.1	41.3	28.8
Bregma	4	94.9 ± 8.3		8.8	
Inion	5	102.8 ± 14.0		13.4	
Distance from PF to:					
Central sulcus**	6	50.9 ± 9.7	43.1 ± 11.4	19.1	26.4
Vertex	7	73.5 ± 14.0		19.0	
Confluence of sinuses	8	84.9 ± 8.2		9.6	
Eurion**	9	72.0 ± 7.2	76.8 ± 7.9	10.7	10.2
Distance from angular gyrus to:					
Parietal foramen**	10	56.9 ± 11.2	64.8 ± 8.1	19.7	14.5
AGyRSS	11	75.1 ± 12.1		16.1	
Area of the squamous part of the occipital bone	12	10,477 ± 1,792		17.0	

Denotes statistically significant results (**p<0.01)

The PF was identified in 83 of the 119 (69.7%) patients studied. Since both parietal bones of each patient were assessed individually, a total of 166 parietal bones were reviewed, of which 122 (73.4%) presented PFs. Of these, 23 were located in the left hemicranium, 21 in the right, and 39 were bilateral cases. The distribution of the 122 foramina is shown in Figure 4. All PFs were situated lateral to the sagittal suture and anterior to the lambda.

There was no significant difference in the relationship of PFs to cranial landmarks between males and females, χ^2 (1, n = 83) = 4.44, p = 0.108. The mean horizontal distance from the obelion to the PF (#2) was 8.86 ± 3.07 mm. The vertical distance from the obelion to the lambda (#1) measured 35.28 ± 6.9 mm, to the bregma (#4) 94.91 ± 8.32 mm, and to the inion (#5) 102.8 ± 13.93 mm (Table 1). The mean horizontal component (#11) of the distance from the PF to the angular gyrus was 75.11 ± 12.1 mm, while the vertical component (#3) showed a significant laterality effect ($p < 0.010$), with mean values of 25.62 ± 10.57 mm on the left and 34.93 ± 10.05 mm on the right (Table 1). Pearson's correlation analysis revealed that parameter #1 was negatively correlated with #6 ($p < 0.05$) and #4 ($p < 0.001$), but positively correlated with #5 ($p < 0.05$).

The relationship between the PF and the SSS (parameter #13) was assessed in axial MRI slices at the level of the PF, within the posterior third of the sagittal suture (Figure 4). The mean distance from the left PF to the left margin of the SSS was 3.73 ± 3.61 mm, while the distance from the right PF to the right margin measured 3.57 ± 3.14 mm. The average width of the SSS was 12.06 ± 3.47 mm (Table 1).

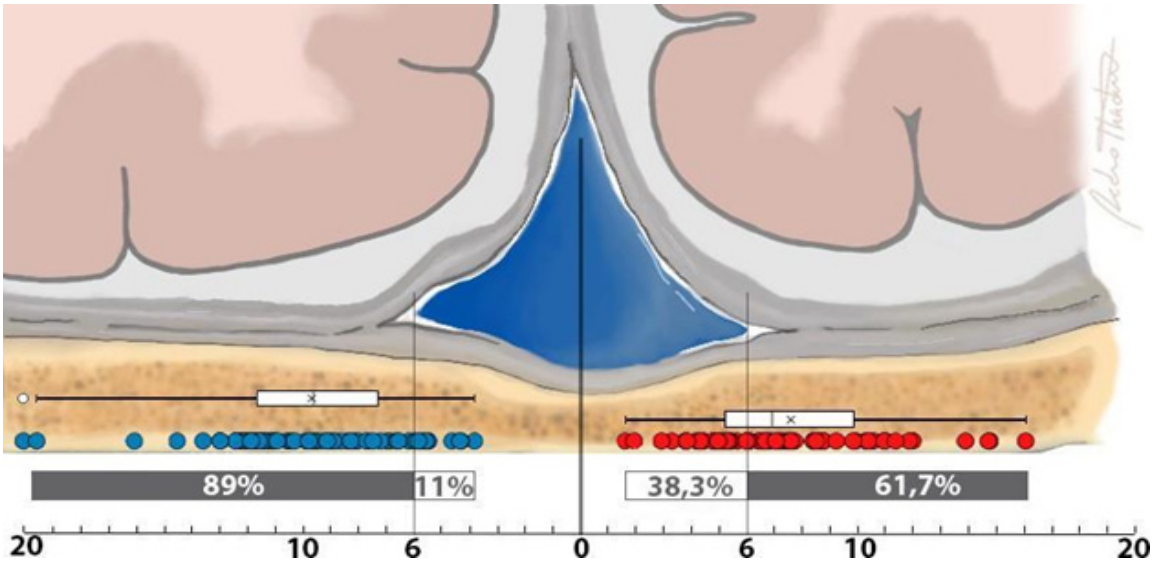

Figure 4. Illustration of the external opening dispersion of the parietal foramina (PF) and their relationship to the superior sagittal sinus (SSS). On the left side, 89% of PFs were located within 14 mm lateral to the left margin of the SSS, while 11% were positioned directly above it. On the right side, 61.7% of PFs were lateral to the right margin of the SSS, whereas 38.3% were directly overlying it. Units in millimeters. 'X' indicates the mean; '|' indicates the median.

Discussion

The PF is a consistent and recognizable anatomical landmark that can be used to localize nearby eloquent structures, both in vivo and on MRI studies (15–17). This can reduce surgical time by increasing accuracy, a benefit that is particularly valuable during emergency procedures and in hospitals where access to reliable neuronavigation systems is limited (18–20). It is also evident that misplacing the craniotomy window directly over the emissary vein can lead to iatrogenic morbidity, either through the risk of superior sagittal sinus (SSS) air embolism or by providing a potential pathway for infections to spread into the cranial cavity (3,4). Therefore, surgeons should remain aware of the PF and take this anatomical variation into consideration during surgical planning and execution.

The present study has characterized the topography of the PF in a Brazilian cohort, and the PFs were identified in 69.7% of cases, consistently located anterior to the lambda and lateral to the sagittal suture. A key strength of our study lies in the use of contrast-enhanced MRI rather than dry skulls, which allowed for more accurate anatomical assessment. This approach confirmed the presence of emissary veins traversing the foramina, ensuring that only true foramina were included in the analysis, while small bone defects without vascular penetration were excluded (4). In addition, we were able to compare different external cranial landmarks to determine which serves as the most reliable reference point for locating the PF.

Inion, bregma, and lambda were used to determine PF location. When considering a 20-mm radius from each parameter's mean value, distinct scatter patterns of PF distribution were observed. Specifically, 92.6% of PFs fell within that radius when measured from the lambda (mean = 35.3 mm), 91.8% from the inion (mean = 102.8 mm), and 90.1% from the bregma (mean = 94.9 mm). These differences may reflect the distinct cranial trajectories implied by each measurement. However, an inverse relationship emerged when analyzing the coefficient of variance: the bregma showed the lowest variability (8.8%), followed by the inion (13.4%) and the lambda (19.6%). Additionally, lambda is rarely palpable in clinical practice, giving both the bregma and inion a practical advantage as they are easily visible and palpable landmarks. A possible explanation for the higher coefficients of variance observed with the lambda and inion, compared to the more stable bregma, lies in the variability of the squamous portion of the occipital bone. In our sample, this area measured on average 10,477 mm², with a coefficient of variance of 17.1%—a value intermediate between those of the inion (13.4%) and lambda (19.6%). This variability impacts the lambda more significantly than the inion, as the lambda lies at the apex of the occipital bone and is influenced by the overall bone height, whereas the inion is positioned in the middle third of the occipital bone, where variation is less pronounced. Additionally, the occasional presence of Wormian bones (sutural bones) within the lambda region can further decrease the accuracy of this landmark for locating the PF (21).

On the other hand, Bruner et al. (22) demonstrated that the distances between the paracentral lobule and the bregma, as well as between the parietal lobe and the lambda, are actively influenced by variations in the size of the precuneal area. Consequently, the relative cranial position of these landmarks to underlying cerebral structures varies as a function of parietal area size (22). These findings indicate that the precise positioning of cerebral parenchymal structures is influenced by multiple factors and does not always correspond directly to external bony landmarks. This potential lack of alignment between brain regions and cranial sutures underscores the need for caution when inferring cortical topography based solely on cranial boundaries (23).

Taken together, these findings suggest that the bregma is a reliable landmark that can be palpated and used to locate the PF in a clinical setting, as the foramen is most often situated within a 20-mm radius from it. Moreover, when the PF does fall within this radius, its positional consistency increases, as reflected by the coefficient of variation. Therefore, studies and surgical procedures should prioritize the bregma as a reference point for identifying the PF.

One particularly interesting finding was that the PF and its emissary veins may serve as a practical landmark for the superior sagittal sinus (SSS), which lies immediately beneath. Contrast-enhanced MR imaging proved valuable for delineating the vascular components of the PF (4,5,8). In this study, the relationship between the PF and the SSS was measured and compared with previous reports describing the anatomical relationships of the SSS to the sagittal suture and to the midline, specifically at the posterior third of the suture (24,25). The correlation between the PF and the SSS was more consistent on the left hemisphere. Among the 62 left PFs identified, 88% were located within 1 cm lateral to the left margin of the SSS. By contrast, the right PFs showed a more heterogeneous distribution: 61.7% were positioned within 1.4 cm lateral to the right margin of the SSS, while 38.3% lay directly over the sinus (Figure 3).

In a cadaveric study of 30 specimens, the SSS was found to deviate to the right of the sagittal suture in 63% of cases, to lie directly beneath the suture in 20%, and to deviate to the left in 17% (24). It appears that the relationship between the SSS and the sagittal suture is less consistent in this cranial region compared with the PF–SSS relationship. Another study reported that the SSS was consistently displaced to one side of the midline, underscoring that the midline itself is not a reliable landmark for identifying the SSS (25). These findings suggest that the PF may serve as a more reliable landmark than both the sagittal suture and the midline for predicting the position of the SSS and for navigating this region. In particular, the left PF appears to provide the most consistent guidance, which could be especially valuable in emergency surgeries by helping surgeons avoid iatrogenic injury.

Computed tomography (CT) can assist physicians in identifying both the emissary vein and the SSS in individual patients, thereby reducing the risk of inadvertent vascular injury. However, in emergency settings or in institutions lacking reliable imaging or neuronavigation equipment, a simpler guideline is warranted. Based on our findings, we propose that surgical incisions made at least 1 cm lateral to the PF can minimize the risk of injuring vascular structures. Even in cases where the PF was directly overlying the SSS (11% on the left and 39% on the right), the margins of the sinus were no closer than 4 mm to the left PF and 8.5 mm to the right PF. This reinforces the PF as a practical anatomical reference to help clinicians avoid vessel damage and potentially fatal hemorrhage.

The small coefficient of variance observed for parameter #8 (9.6%) suggests a vascular influence on PF positioning, possibly related to the confluence of sinuses or adjacent venous structures that contribute to the formation of the emissary vein. This valveless vein plays an important physiological role in regulating intracranial pressure and brain temperature, owing to its capacity for bidirectional blood flow between the intracranial and extracranial compartments. Given that scalp temperature is generally lower than intracranial temperature, this venous exchange may serve as a mechanism to regulate intradural temperature.

Furthermore, in patients with parasagittal meningiomas, the emissary vein may contribute to tumor drainage. In addition, this venous channel can serve as an access route for the embolization of dural vessels, providing both diagnostic and therapeutic opportunities in selected cases (26). Therefore, accurate localization of the PF and its emissary vein on radiological studies, followed by careful management or targeted obstruction of the emissary vein, may help reduce intraoperative blood loss and minimize the risk of injury to the SSS. Awareness of the PF and its venous connections is not only essential for preventing iatrogenic complications, but may also open avenues for the development of new therapeutic strategies.

The angular gyrus is a functionally asymmetric cortical region that is consistently activated across a wide variety of cognitive tasks. Damage to the left angular gyrus has a profound impact on language and word processing, whereas stimulation of the right angular gyrus has been shown to induce out-of-body experiences (27,28). Hence, careful surgical maneuvering in this region is essential. Anatomical asymmetry in laterality was also observed. When measured from the obelion to the angular gyrus reference point on the sagittal suture (parameter #3), the right angular gyrus (34.9 ± 10.6 mm) was positioned more anteriorly than the left (25.6 ± 10.1 mm). Conversely, the lateral distance between the angular gyrus reference point on the sagittal suture and the angular gyrus itself averaged 75.1 mm (18,19,29,30).

This study has some limitations. First, the number of specimens was insufficient to establish the true prevalence of PF in the Brazilian population. Second, our analysis was limited to Brazilian patients. Given the well-documented anatomical variations in cranial morphology across different populations, results may differ in other ethnic groups. Finally, age-related changes in bony structures could also influence the measurements, which were not stratified by age in the present study (31). Moreover, the topography of the PF in our study was derived predominantly from elderly subjects (mean age 58.9 years), which may not reflect the anatomical characteristics of younger individuals, particularly pediatric patients. Age-related changes in cranial morphology could influence PF positioning and frequency. Therefore, future studies with larger and more diverse samples, including different age groups and populations from various regions of the world, are warranted to clarify potential age- and race-related variations.

In conclusion, based on our findings and prior reports, the high prevalence of the PF underscores the importance of recognizing this anatomical variation when performing surgical or invasive procedures in the parietal region. This is particularly relevant in interventions requiring careful maneuvering around the SSS, for which the PF appears to serve as a reliable landmark. Among the external cranial references, the bregma emerged as the most stable and accurate landmark for localizing the PF. Standardizing a method for PF localization may assist surgeons in planning parietal craniotomies, help prevent iatrogenic injury to the SSS, and facilitate future studies on the anatomical correlations of the PF.

References

1. Gusmão S, Silveira RL, Arantes A. Pontos referenciais nos acessos cranianos. Arq Neuropsiquiatr 2003;61:305–8. Doi:10.1590/S0004-282X2003000200030.
2. Penteado C V, Santo Neto H. The number and location of the parietal foramen in human skulls. Anat Anz 1985;158:39–41.
3. Tsutsumi S, Nonaka S, Ono H, Yasumoto Y. The extracranial to intracranial anastomotic channel through the parietal foramen: delineation with magnetic resonance imaging. Surgical and Radiologic Anatomy 2016;38:455–9. Doi:10.1007/s00276-015-1579-4.
4. Mortazavi MM, Shane Tubbs R, Riech S, Verma K, Shoja MM, Zurada A, et al. Anatomy and Pathology of the Cranial Emissary Veins. Neurosurgery 2012;70:1312–9. Doi:10.1227/NEU.0b013e31824388f8.
5. Freire AR, Rossi AC, de Oliveira VCS, Prado FB, Caria PHF, Botacin PR. Emissary Foramens of the Human Skull: Anatomical Characteristics and its Relations with Clinical Neurosurgery. International Journal of Morphology 2013;31:287–92. Doi:10.4067/S0717-95022013000100045.
6. Tubbs RS, Smyth MD, Oakes WJ. Parietal Foramina Are Not Synonymous with Giant Parietal Foramina. Pediatr Neurosurg 2003;39:216–7. Doi:10.1159/000072475.
7. Currarino G. Normal variants and congenital anomalies in the region of the obelion. American Journal of Roentgenology 1976;127:487–94. Doi:10.2214/ajr.127.3.487.
8. Yoshioka N, Rhoton AL, Abe H. Scalp to Meningeal Arterial Anastomosis in the Parietal Foramen. Operative Neurosurgery 2006;58:ONS-123-ONS-126. Doi:10.1227/01.NEU.0000193516.46104.27.
9. Ferreira MR de S. Morfometria dos forames emissários parietais: prevalência e variações relacionadas ao sexo. Dissertacion. Federal University of Pernambuco, 2018.
10. Collipal E, Silva H, Quintas F, Martínez C, del Sol M. Estudio Morfométrico del Foramen Parietal. International Journal of Morphology 2009;27. Doi:10.4067/S0717-95022009000200028.
11. Irmak MK, Korkmaz A, Erogul O. Selective brain cooling seems to be a mechanism leading to human craniofacial diversity observed in different geographical regions. Med Hypotheses 2004;63:974–9. Doi:10.1016/j.mehy.2004.05.003.
12. Cabanac M, Brinnel H. Blood flow in the emissary veins of the human head during hyperthermia. Eur J Appl Physiol Occup Physiol 1985;54:172–6. Doi:10.1007/BF02335925.
13. Falk D. Evolution of cranial blood drainage in hominids: Enlarged occipital/marginal sinuses and emissary foramina. Am J Phys Anthropol 1986;70:311–24. Doi:10.1002/ajpa.1330700306.
14. Brace, C. L. [Review of The Evolution of Homo erectus: Comparative Anatomical Studies of an Extinct Human

Species, by G. P. Rightmire]. Human Biology, 1991; 63(6), 883–886. http://www.jstor.org/stable/41464238.
15. Cotton F, Rozzi FR, Vallee B, Pachai C, Hermier M, Guihard-Costa A-M, et al. Cranial sutures and craniometric points detected on MRI. Surgical and Radiologic Anatomy 2005;27:64–70. Doi:10.1007/s00276-004-0283-6.
16. Salamon N, Sicotte N, Mongkolwat P, Shattuck D, Salamon G. The human cerebral cortex on MRI: value of the coronal plane. Surgical and Radiologic Anatomy 2005;27:431–43. Doi:10.1007/s00276-005-0022-7.
17. Juerchott A, Saleem MA, Hilgenfeld T, Freudlsperger C, Zingler S, Lux CJ, et al. 3D cephalometric analysis using Magnetic Resonance Imaging: validation of accuracy and reproducibility. Sci Rep 2018;8:13029. Doi:10.1038/s41598-018-31384-8.
18. Campero A, Ajler P, Emmerich J, Goldschmidt E, Martins C, Rhoton A. Brain sulci and gyri: A practical anatomical review. Journal of Clinical Neuroscience 2014;21:2219–25. Doi:10.1016/j.jocn.2014.02.024.
19. Wild HM, Heckemann RA, Studholme C, Hammers A. Gyri of the human parietal lobe: Volumes, spatial extents, automatic labelling, and probabilistic atlases. PLoS One 2017;12:e0180866. Doi:10.1371/journal.pone.0180866.
20. Ahdab R, Ayache SS, Farhat WH, Mylius V, Schmidt S, Brugières P, et al. Reappraisal of the anatomical landmarks of motor and premotor cortical regions for image-guided brain navigation in TMS practice. Hum Brain Mapp 2014;35:2435–47. Doi:10.1002/hbm.22339.
21. Kumar T.M V, Kumar V, Yadav N. The occurrence of wormian bones within the cranial sutures and their clinical significance. International Journal of Anatomy and Research 2016;4:3082–6. Doi:10.16965/ijar.2016.408.
22. Bruner E, Amano H, de la Cuétara JM, Ogihara N. The brain and the braincase: a spatial analysis on the midsagittal pro file in adult humans. J Anat 2015;227:268–76. Doi:10.1111/joa.12355.
23. Jiang X, Iseki S, Maxson RE, Sucov HM, Morriss-Kay GM. Tissue Origins and Interactions in the Mammalian Skull Vault. Dev Biol 2002;241:106–16. Doi:10.1006/dbio.2001.0487.
24. Tubbs RS, Salter G, Elton S, Grabb PA, Oakes WJ. Sagittal suture as an external landmark for the superior sagittal sinus. J Neurosurg 2001;94:985–7. Doi:10.3171/jns.2001.94.6.0985.
25. Reis CV, Gusmão SebastiãoNS, Elhadi A, Dru A, Tazinaffo U, Zabramski J, et al. Midline as a landmark for the position of the superior sagittal sinus on the cranial vault: An anatomical and imaging study. Surg Neurol Int 2015;6:121. Doi:10.4103/2152-7806.161241.
26. Nawashiro H, Nawashiro T, Nawashiro A. Subcutaneous Extension of Parasagittal Atypical Meningioma Through Parietal Foramen. World Neurosurg 2019;125:104–5. Doi:10.1016/j.wneu.2019.01.185.
27. Seghier ML. The Angular Gyrus. The Neuroscientist 2013;19:43–61. Doi:10.1177/1073858412440596.
28. Kurimoto M, Asahi T, Shibata T, Takashi C, Nagai S, Hayashi N, et al. Safe Removal of Glioblastoma Near the Angular Gyrus by Awake Surgery Preserving Calculation Ability-Case Report-. Neurol Med Chir (Tokyo) 2006;46:46–50. Doi:10.2176/nmc.46.46.
29. Rusconi E. Gerstmann syndrome: historic and current perspectives, 2018, p. 395–411. Doi:10.1016/B978-0-444-63622-5.00020-6.
30. Lerch JP, van der Kouwe AJW, Raznahan A, Paus T, Johansen-Berg H, Miller KL, et al. Studying neuroanatomy using MRI. Nat Neurosci 2017;20:314–26. Doi:10.1038/nn.4501.
31. Urban JE, Weaver AA, Lillie EM, Maldjian JA, Whitlow CT, Stitzel JD. Evaluation of morphological changes in the adult skull with age and sex. J Anat 2016;229:838–46. Doi:10.1111/joa.12247.

Data availability: The datasets generated and/or analyzed during the current study are available from the corresponding author upon reasonable request.

Acknowledgements
This research was supported by the institutional program of grants for scientific initiation through the Conselho Nacional de Desenvolvimento Científico e Tecnológico (CNPq) funded by the Brazilian government. Mr Austin Post for inspiring this study. Dr. João Brainer for supporting this study.
Preprint: The present article was initially made available as a preprint (Parietal Foramen as A Landmark to Locate Intracranial Vascular and Parenchymal Structures, DOI: 10.21203/rs.3.rs-114662/v1).
Authors contribution: Pedro BL: analyzed and interpreted the data, wrote the manuscript and illustrated all the figures; MMV: designed this study, wrote the manuscript; MRF: helped design this study and wrote it; ABL: analyzed the data; Paulo BL: revised this manuscript.
Conflict of interest: The authors declare no competing interests.
Funding: This research did not receive funding.

Pedro Brainer-Lima
https://orcid.org/0000-0003-0819-0155
Alessandra Brainer-Lima
https://orcid.org/0000-0003-0096-4101
Maria Rosana Ferreira
https://orcid.org/0000-0003-1166-5342
Paulo Brainer-Lima
https://orcid.org/0009-0004-4842-7879
Marcelo Moraes Valença
https://orcid.org/0000-0003-0678-3782